Approaches to structure and dynamics of biological systems by electron-paramagnetic-resonance spectroscopy

Scarpelli, F.

Chapter 3. Dynamics of surface spin labels in cytochrome c peroxidase studied by EPR

3.1 Introduction

Site-directed spin labeling (SDSL) has become a powerful tool for studying dynamics and conformational changes of proteins [1-3]. The basic procedure of SDSL consists in the substitution of a selected amino acid for a cysteine, followed by the modification of the reactive SH group with a selective nitroxide agent [1]. One of the most used nitroxides is the methanethiosulfonate spin label (MTSL), see Fig. 1. When studied by electron paramagnetic resonance (EPR), the analysis of the line shape of the spectra provides information about the dynamics of the nitroxide. This information is relevant because the nitroxide mobility reflects the dynamics of its binding site, such as backbone and side chains, and, in certain cases, of the whole protein.

Previous studies addressed the mobility of spin labels at sites ranging from buried to surface exposed. Here we investigate spin labels at the surface of a protein. Surface residues have the advantage that the spin labeling is easier, because the cysteine is easily accessible. Spin labels at the surface do not perturb the protein structure. They can give information about the protein surface [4] and about the interaction of the protein with its partners [5,6]. Information about which residues to target when searching for surface sites can come from the X-ray structure of the protein using solvent accessibility data [7]. Modeling the possible conformations of the spin label [8-10] is another approach.

Several methods to determine mobility from EPR spectra have been applied in the past [9,11-13]. Recently, the EasySpin-simulation program [14] has become wide spread, but it was not applied systematically to investigate mobility differences of protein spin labels. The simulations yield the rotation-correlation time (τ_c) of the spin labels.

In the present account we compare the simulation approach with the method of line-shape analysis proposed by the Hubbell group [15]. To investigate how well methods using the X-ray structure of a protein can

predict mobile, exposed surface sites, we compare the mobility results to the prediction of solvent accessibility [7] and conformational freedom [16].

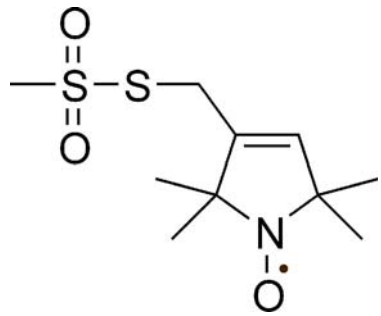

Fig. 4: Chemical structure of a nitroxide spin-label. The black dot represents the unpaired electron.

This is performed for ten spin-labeled surface sites of the cytochrome c peroxidase (CcP) protein. The mobility is measured by continuous-wave (cw) EPR in solution. We find that for surface residues with small mobility differences, the τ_c values give a better differentiation than the Hubbell model and that the conformational model [6,17] works well to predict mobilities.

3.2 Materials and Methods

3.2.1 Sample preparation

In order to prepare single-cysteine CcP variants, site-directed mutagenesis was carried out using the Quik Change™ polymerase chain reaction protocol (Stratagene, La Jolla, CA) with the plasmid CCP(MKT) as a template [18]. All constructs were verified by DNA sequencing. The CcP variants were expressed in E. coli and purified following the published procedures [18-20]. Concentrations of five-coordinated high-spin ferric CcP, used in this work, were determined from the optical absorbance at 410 nm (ε = 106.1 mM^{-1} cm^{-1}) [21] and at 408 nm (ε = 98 mM^{-1} cm^{-1}) [22], respectively.

Purified single-cysteine CcP variants were incubated with 10 mM DTT in 0.1 M Tris-HCl (pH 8.0), with 0.1 M NaCl for 2 hours at room temperature, in order to reduce intermolecular disulfide bonds. The DTT was removed by passing the CcP solution through a PD-10 column (Amersham Pharmacia, Uppsala, Sweden). The resulting monomeric protein was reacted with a 7 to 10-fold excess of MTSL and incubated overnight at room temperature.
The label MTSL [(1-oxyl-2,2,5,5-tetramethyl-3-pyrroline-3-methyl)-methanethiosulfonate] was purchased from Toronto Research Chemicals (North York, ON, Canada) and used without further purification. Upon completion of the reaction, the protein solution was passed through a PD-10 column to remove any unreacted label, followed by exchange into 20 mM NaPi and 0.1 M NaCl (pH 6.0), and concentrated by ultracentrifugation using Amicon Ultra concentrators (Millipore, Billerica, MA).

3.2.2 EPR experiments

The X-band cw EPR measurements have been performed at room temperature using an ELEXSYS E 680 spectrometer (Bruker Biospin, Rheinstetten, Germany) equipped with a rectangular cavity. All measurements were performed in solution and capillaries of 1.3 mm inner diameter were used. The sample concentrations varied from 0.2 to 0.5 mM. All spectra were acquired using a modulation frequency of 100 kHz, a modulation amplitude of 0.1 mT and a microwave attenuation of at least 25 dB. The time to acquire each spectrum was up to 30 minutes. All spectra were baseline corrected by subtraction of a polynomial of first order, using the Xepr software (Bruker Biospin, Rheinstetten, Germany).
The proteins with a spin label at positions 38, 137, 200 and 288 have been measured previously, by Alex Volkov, on a Bruker ELEXSYS E 680 (Bruker Biospin, Rheinstetten, Germany) with the following parameters: modulation frequency 100 KHz, modulation amplitude 0.15 mT, microwave attenuation at least 25 dB and 5 to 25 scans [17].

3.2.3 Simulation of the EPR spectra

The EPR spectra have been simulated using *EasySpin 2.7.1* [14]. For all

simulations the following tensor values were used: G = [g_{xx} g_{yy} g_{zz}] = [2.00906 2.00687 2.003] [23]; A = [A_{xx} A_{yy} A_{zz}] = [13 13 109] MHz. The line width used in the simulation of the model spectra is: 0.1 mT for the spectra simulated with τ_c values that vary from 1.00 ns to 1.55 ns; 0.4 mT for τ_c values from 2 to 3.6 ns; 1 mT for τ_c values from 4 ns to 15 ns.

3.2.4 Second-moment analysis

The line width of the EPR spectra depends amongst other factors on the dynamics. The second moment of the spectrum used to quantify this, was calculated according to the following equation

$$<\Delta B^2> = \frac{\int (B - B_F)^2 S(B) dB}{\int S(B) dB}, \quad (1)$$

where *S(B)* is the absorption spectrum, B_F and *B* are the first moment and the magnetic field, respectively. The absorption EPR spectra were baseline corrected using the Xepr software (Bruker Biospin, Rheinstetten, Germany) and the first and second moments were calculated numerically using MatLab (MathWorks, MA, USA). The calculated $<\Delta B^2>$ value is affected by the baseline correction and the signal-to-noise ratio of the EPR spectrum of each sample. Therefore, the value of the second moment has an error that varies between 6 % and 9 %.

3.2.5 Width of the central line

The width of the central line (ΔB) has been measured by taking the separation between the two peaks of the central line of the first-derivative EPR spectra. The presence of free spin labels affects the central line, making it sharper. This results in a smaller separation between the two peaks of the central line. Each sample has a different amount of free spin label. To minimize the error in ΔB, we have subtracted a spectrum of a free spin label from the experimental spectrum. The error in ΔB that results from this procedure varies between 9 % and 16 %.

3.2.6 Conformational model

To characterize the mobility of the nitroxide spin label attached to the surface of the CcP, all the possible orientations of the MTSL have been considered [6]. To generate these, the attached MTSL was systematically rotated around the five single bonds that join its ring to the C_α atom of the cysteine and only the sterically allowed conformers were retained for each mutant [17].

3.2.7 Solvent-accessible surface

The solvent-accessible surface has been calculated as the fractional solvent accessibility (f_{SA}). It consists of the ratio of the solvent-accessibility surface of a free residue and the solvent-accessibility surface of the same residue attached to the protein structure. The fractional solvent accessibility (f_{SA}) for native residues in CcP was computed from the crystal structure, taken from the PDB entry 2PCC [24], using the program MolMol [25] and a probe radius of 1.4 Å.

3.2.8 Protein rotation-correlation time

The rotation-correlation time of the CcP protein has been calculated from the Einstein-Stokes equation [26]

$$\tau_c = \frac{4\pi\eta_s r_h^3}{3k_B T}, \tag{2}$$

where η_s is the viscosity of the solution in centipoises, k_B the Boltzmann constant, T the temperature, and r_h the hydrodynamic radius of the protein, which was estimated according to [26]

$$r_h = \sqrt[3]{\frac{3\bar{V}M_r}{4\pi N_A}} + r_w, \tag{3}$$

where $\overline{V}$ is the specific volume of the protein, M_r is the molecular weight of the protein, N_A is the Avogadro number and r_w is the hydration radius. Assuming $\overline{V}$ = 0.73 cm^3/g, r_w = 1.6 Å and M_r = 34.2 KDa, Eq. 3 results in r_h = 5 Å. Substituting this radius into Eq. 2 and assuming η_s = η_s (0.1 M NaCl) = 1.013 centipoises [26] yields a τ_c of 12 ns.

3.3 Results

The EPR spectra of ten CcP's spin labeled at different sites (Fig. 2) have been measured at room temperature. All EPR spectra were simulated using *EasySpin* (see materials and methods). The τ_c values obtained from the simulations are given in Tab. 1.

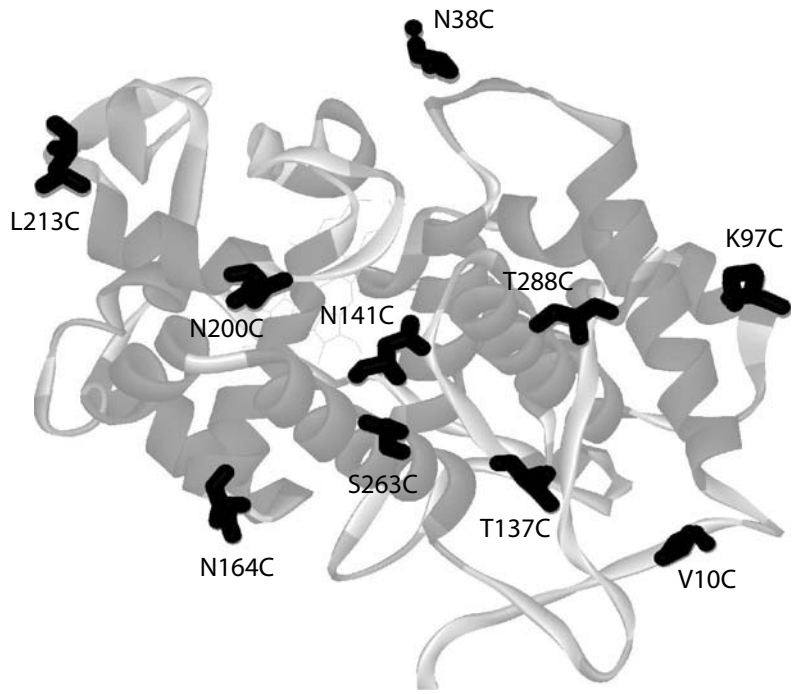

Fig. 2: Ribbon representation of the cytochrome *c* peroxidase (PDB entry 2PCC). The named residues indicate the mutated sites.

Table 1

Parameters form the simulation (τ_c), line shape analysis ($<\Delta B^2>$, ΔB), number of conformations, solvent- accessible surface and structures of ten different spin labeled sites of the Cytochrome *c* peroxidase protein.

Sample	τ_{cs} (ns) *#	τ_{cl} (ns) *#	Second moment $<\Delta B^2>$ (T^2) ¶	Line width ΔB (T) †	Number of conformations	Fractional solvent accessibility
K97C	1.1 (99%)	--	$2.3*10^{-6}$	$2.3*10^{-4}$	1897	0.48
N164C	1.3 (99%)	--	$2.3*10^{-6}$	$2.8*10^{-4}$	1071	0.33
N38C	1.1 (78%)	12.0 (20%)	$2.3*10^{-6}$	$2.2*10^{-4}$	1760	0.53
T137C	1.2 (72%)	12.0 (26%)	$2.4*10^{-6}$	$2.2*10^{-4}$	655	0.24
N141C	1.1 (65%)	12.0 (28%)	$2.4*10^{-6}$	$2.1*10^{-4}$	633	0.29
V10C	1.1 (66%)	12.0 (30%)	$2.4*10^{-6}$	$2.1*10^{-4}$	567	0.23
L213C	1.3 (66%)	12.0 (32%)	$2.7*10^{-6}$	$2.6*10^{-4}$	382	0.27
S263C	1.3 (66%)	12.0 (33%)	$2.7*10^{-6}$	$2.5*10^{-4}$	344	0.10
N200C	1.2 (59%)	12.0 (40%)	$2.6*10^{-6}$	$2.4*10^{-4}$	183	0.08
T288C	1.5 (9%)	12.0 (90%)	$2.9*10^{-6}$	$3.1*10^{-4}$	29	0.07

* The rotation correlation time (τ_c) error is ± 0.1 ns

† The central line- width (ΔB) error varies between 9 % and 16 %

¶ The second moment $<\Delta B_i^2>$ error varies between 6 % and 9 %

The weight error is ± 0.6% (± 3% for the position 137)

For two spin-labeled sites, N164C and K97C, the EPR spectra could be simulated using a single τ_c of about 10^{-9} s. All the other spectra have a multi-component line shape. Each spectrum can be described as the sum of two spectra, each simulated with a single τ_c value. The best agreement with the experimental spectrum is obtained using different weights of the two spectra (Tab. 1). The simulations of the multi-component spectra do

not have a unique solution. Adequate simulations are possible using different combinations of the weights and the τ_c values. We have chosen to fix one τ_c at 12 ns (Tab. 1) for all the multi-component spectra, a value that corresponds to the predicted rotation-correlation time of the protein. Examples of experimental and simulated EPR spectra are shown in Fig. 3, where the spectra *a* and *c* concern the K97C and T288C mutants, which carry respectively the most mobile and the least mobile spin label.

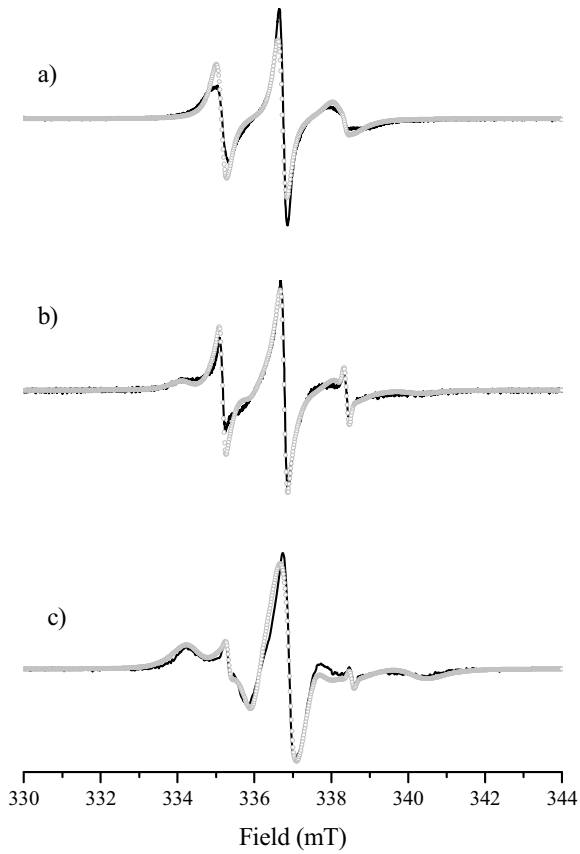

Fig. 3: The cw EPR spectra of cytochrome *c* peroxidase spin labeled at three different positions (black lines) and their simulations (gray circles). a) spin label at position 97; b) spin label at position 213; c) spin label at position 288.

Additionally, a fast component with a τ_c of about 10^{-11} s is required in the simulations. This is attributed to a small fraction of free MTSL, which varies between 1 % and 8 %.
Another approach to classify the mobility of spin labels has been proposed by Hubbell and coworkers [7,15]. It combines the peak-to-peak width of the central line in the first derivative EPR spectra (ΔB) and the second moment ($<\Delta B^2>$) (see materials and methods). At X-band frequency, ΔB and $<\Delta B^2>$ values are determined mostly by the degree of averaging of the *g* and *A* tensors. As the rotation of the nitroxide spin label slows down, the value of $<\Delta B^2>$ and ΔB increases. Thus, these parameters can be used as a measure of the mobility of the nitroxide [7,15,27]. Hubbell and coworkers plot the reciprocal of $<\Delta B^2>$ as a function of the reciprocal of ΔB to characterize the motion of the spin label attached at different sites of a protein [7,15]. The ΔB and $<\Delta B^2>$ values obtained from the EPR spectra of all the spin-labeled mutants measured in this study are summarized in Tab. 1.

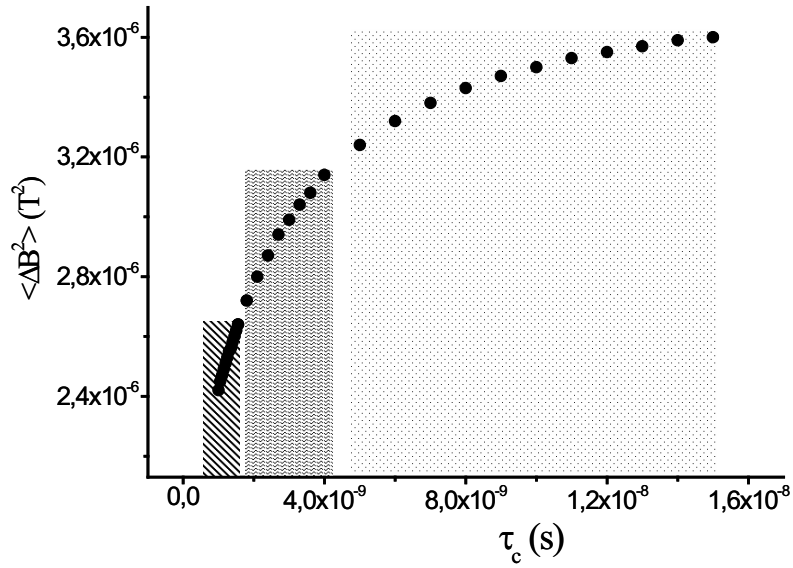

Fig. 4: The second moment ($<\Delta B^2>$) calculated from the model spectra as a function of τ_c. The regions filled with different patterns indicate, from left to right, respectively the short, intermediate and long τ_c used to simulate the model spectra.

To find a link between the ΔB and $\langle \Delta B^2 \rangle$ values and τ_c, EPR spectra of nitroxide spin labels have been simulated for τ_c values between 1 ns and 15 ns. From these simulated spectra, ΔB and $\langle \Delta B^2 \rangle$ were calculated, and graphs of $\langle \Delta B^2 \rangle$ and ΔB as a function of τ_c are shown in Fig. 4 and 5. Regions corresponding to large, intermediate and small values of τ_c are indicated. The width of the central line increases significantly for fast and intermediate τ_c and remains almost constant for τ_c between 4 and 15 ns. This means that ΔB can not add any further information about the spin label mobility for τ_c values bigger than 4 ns. The graph of $\langle \Delta B^2 \rangle$ as a function of τ_c shows that also the second moment increases significantly for short and intermediate τ_c, but continues to increase for τ_c longer than 4 ns, although to a lesser extent. The reciprocal $\langle \Delta B^2 \rangle$ as a function of the reciprocal ΔB calculated from the experimental EPR spectra and from the model spectra are summarized in Fig. 6.

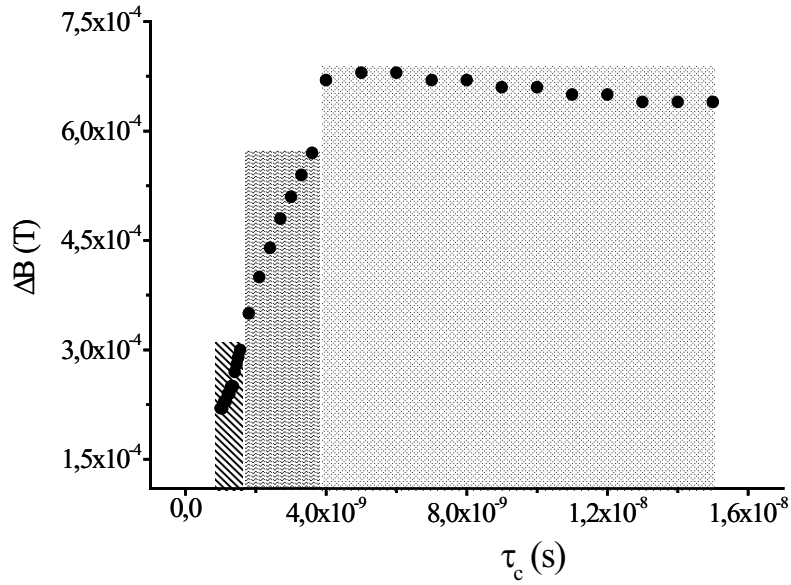

Fig. 5: The width of the central line (ΔB) of the model spectra as a function of τ_c. The regions filled with different patterns indicate, from left to right, respectively the short, intermediate and long τ_c used to simulate the model spectra.

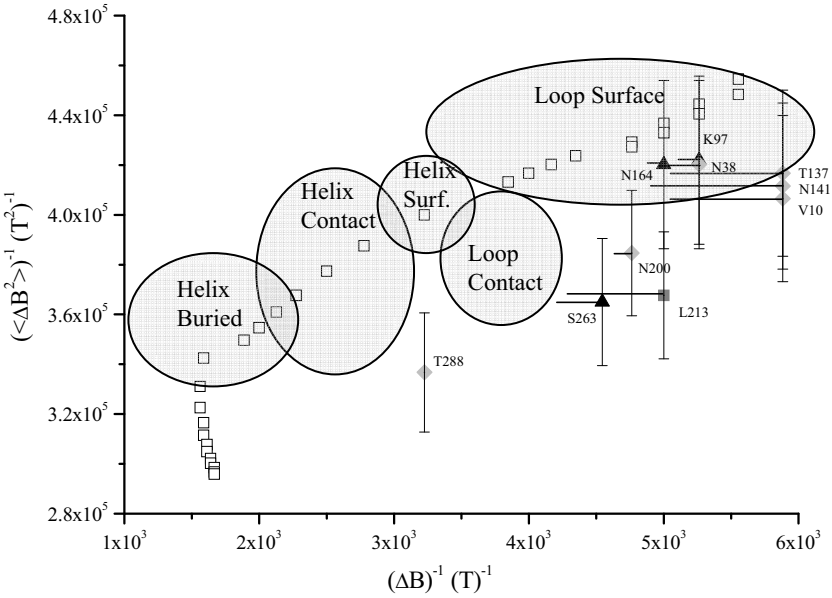

Fig. 6: The reciprocal of $<\Delta B^2>$ as a function of the reciprocal of ΔB from the experimental EPR spectra (symbols with the mutant labels) and from the model spectra (black empty squares). The triangles represent the values calculated from the spectra of the spin labels attached to a helical region, the diamonds of the spin labels attached to a loop region and the black square of the spin label attached to a β-sheet. The gray regions represent secondary structure regions in the Hubbell mobility map [7]. The source of the errors is discussed in Materials and Methods.

The buriedness of a protein residue can be quantified through the solvent accessibility, calculated as the fractional solvent accessibility (f_{SA}, see materials and methods). Hubbell and coworkers used the f_{SA} values to classify the location of the residues in the protein structure [7]. They established that residues with an $f_{SA} \leq 0.05$ can be considered as "buried", those with an f_{SA} between 0.05 and 0.25 as "partially solvent-accessible" and those with an $f_{SA} > 0.25$ as "solvent-accessible". The f_{SA} value for each native residue, which will be replaced by the cysteine to which the spin label binds, is reported in Tab. 1.
In Fig. 7, the solvent accessible surface area for the residues at position 97, 213 and 288 is shown.

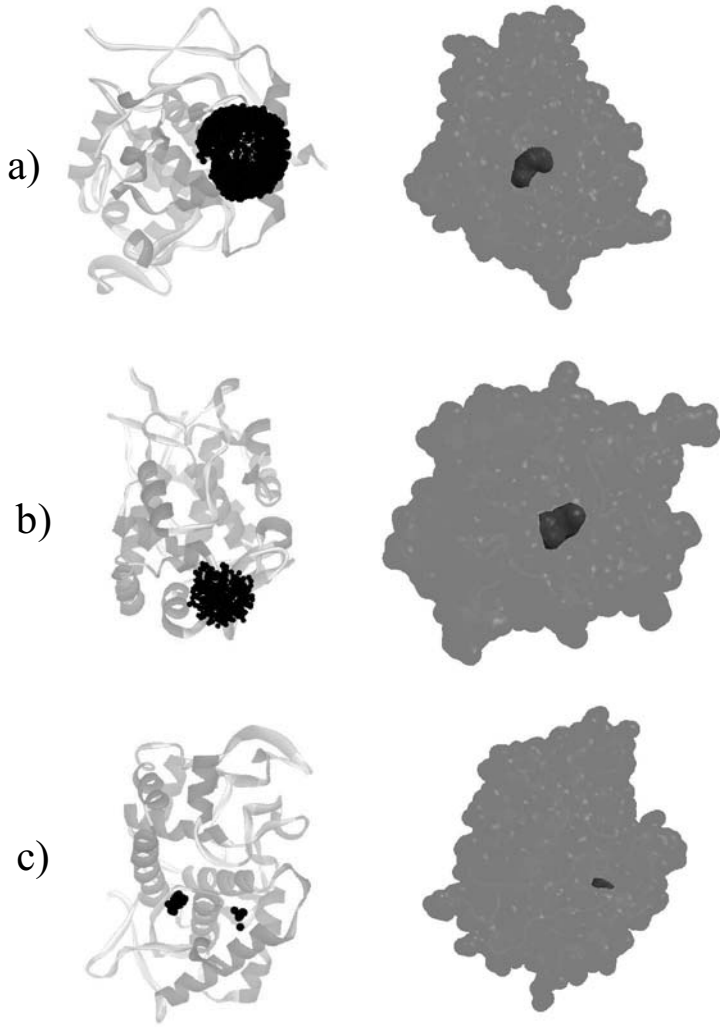

Fig. 7: Left: allowed conformations of the nitroxide spin label shown as black dots at the position of the nitroxide oxygen atom for a spin label at position (a) 97, (b) 213, and (c) 288. Right: solvent accessible surface for these residues.

In order to better understand and interpret the mobility of the nitroxide we make use of the results of the model by Volkov et al [6,17]. This model takes into account the rotational degrees of freedom of the single bonds linking the spin label to the protein backbone. It yields an ensemble of conformations which are represented by the positions of the oxygen atom of the MTSL (see Fig. 7). For our interpretation we use the number of conformations derived from the model (Tab. 1). The number of possible conformations of the spin label varies from 29 for the mutant T288C to 1897 for K97C mutant, see Tab. 1 and Fig. 7.

3.4 Discussion

The goal of this study was to use EPR to investigate the mobility of spin labels attached to ten different sites on the surface of the CcP protein.

From the τ_c values in Tab. 1, the mutants can be divided into two groups: the mutants K97C and N164C that are characterized by a single τ_c value (τ_{cs}), and the other eight mutants which, in addition to τ_{cs}, have a long τ_c (τ_{cl}).

For the mutants with two τ_c values, there must be two populations of spin labels: one corresponding to τ_{cs}, where the spin label is almost freely rotating around the bonds linking it to the protein backbone, and one corresponding to τ_{cl}, in which the motion of the spin label is more restricted. If the rotation of the spin label around the bonds linking it to the protein backbone is longer than or equal to the τ_c of the protein, the τ_c observed will be that of the protein itself. Therefore a τ_c value of 12 ns has been chosen for the second component in the simulation, corresponding to the predicted rotational-correlation time of the CcP protein (materials and methods). With the exception of the T288C mutant, the dominant contribution to the spectra comes from the τ_{cs} component. The magnitude of τ_{cs}, between 1.1 and 1.5 ns agrees well with the τ_c values of the surface residues reported by White et al. [5].

In Tab. 1, the mutants are ordered according to the mobility. The single component spectra are ordered according to τ_{cs}. For the mutants with multi-component EPR spectra, which all have the same τ_{cl} of 12 ns, the

order has been chosen according to the weight of the spectral component with the τ_{cl}. This weight varies from 20 % for N38C mutant to 90 % for T288C. A unique order is established and only the pairs T137C/N141C and L213C/S263C have values too close to be distinguished.

An alternative approach to describe the mobility of spin labels has been put forward by Hubbell and coworkers. In their model, a graph of the reciprocal $<\Delta B^2>$ values as a function of the reciprocal ΔB [7,15] serves to classify residues according to mobility and to define the secondary structure of the protein at the site of the spin label. To do so, different regions in the mobility map were defined (gray areas in Fig. 6). For example, spin labels at loop/surface sites should have the biggest values of both $<\Delta B^2>^{-1}$ and ΔB^{-1} (upper-right region of the graph in Fig.6) which correspond to highest mobility. The helix/surface, the loop/contact and the helix/contact spin labeled sites have $<\Delta B^2>^{-1}$ and ΔB^{-1} values that suggest an intermediate mobility of the attached spin label (central region of the graph in Fig. 6). The helix/buried spin labeled sites have the smallest $<\Delta B^2>^{-1}$ and ΔB^{-1} values (lower-left region of the graph in Fig. 6), which correspond to the lowest mobility.

In order to assign which τ_c values correspond to which mobility region, data points from model spectra are compared to the Hubbell mobility map (Fig. 6). Overall, the data points, simulated with a range of τ_c values, follow the trend of the Hubbell mobility regions. The loop/surface region (upper-right part of the Hubbell graph) corresponds to τ_c values that vary between 1 ns and 1.5 ns, i.e., the most mobile spin labels. The helix/surface, the loop/ contact and the helix/contact of the Hubbell map (central part of the graph) correspond to τ_c values between 1.8 ns and 3.6 ns and represent the spin labels with intermediate mobility. The helix/buried region (lower-left part of the graph) corresponds to τ_c values between 4 ns and 15 ns and represents the least mobile spin labels. There is a good correspondence of the mobility criteria given for the Hubbell graph and the τ_c values, showing that, with respect to single component spectra, the two approaches are equivalent. The τ_c values assigned to the regions were obtained for single-component-model spectra. For multi-component spectra, where slow and fast mobility components are present, there will be cases that have a different combination of $<\Delta B^2>$ and ΔB values than those of single-component spectra. The ΔB value that is sensitive to the sharpness of the

central line will be affected only by the fast τ_c value. On the other hand, $<\Delta B^2>$, which is sensitive to the broadness of the spectrum, will be dominated by the effect of the slow τ_c values [15]. This means that the data points obtained from multi-component spectra can be outside the narrow band defined by the single component spectra (empty squares in Fig. 6).
The experimental data points for the surface spin labels of CcP are shown in Fig. 6. The six most mobile spin labels (at position 164, 97, 38, 137, 141 and 10) cluster in the vicinity of the loop surface region. Given the experimental error, no mobility differences can be discerned within this group. Another group comprises the spin labels at position 200, 213 and 263. From the region occupied by these data points they are less mobile than the previous six. Finally, the data point that corresponds to the spin label at position 288 is the most immobilized according to the Hubbell plot (Fig. 6). The three groups can be interpreted as Hubbell regions. The first group overlaps the loop-region of the Hubbell plot (Fig. 6) of the protein annexin [7], but the remaining mutants are outside these regions. Such a variation in the position where the regions occur has been found before [7,27]. The spin-labeled residues that belong to secondary structure elements (PDB entry 2PCC [24]) classified as loop, helical and β-sheet sites occur in almost every region, showing that for surface spin labels the secondary structure of the site is not relevant for mobility. This is similar to the results found for the spin-labeled annexin [7], but different from those for the spin-labeled SNAP-25 [27].
In the following, the mobility as obtained from the τ_c values, will be interpreted in terms of the structure of the protein. The solvent accessibility of a residue, expressed in the f_{SA} value, reveals how much a given residue is exposed to the environment. A large solvent accessibility should correspond to high mobility. The f_{SA} values show that half of the residues investigated in this study are solvent accessible, the other half partially-solvent accessible. The ranking of the f_{SA} values deviates in several aspects from the one derived from the τ_c values, showing that the predictive value of the f_{SA} values is limited.
The number of conformations derived from the model by Volkov et al. [6,17] is related to the mobility of the spin labels. A larger number of conformations means a more flexible and mobile spin label. The spin label at position 97, the most mobile site in the experiment, has the largest number of conformations. The other extreme is the spin label at position 288, which has the lowest number of conformations. The pairs

T137C/N141C and L213C/S263C, which have similar τ_c characteristics also have a similar number of conformations (Tab. 1). Thus, qualitatively the number of conformations follows the trend of the τ_c values suggesting that the model is a proper indicator for mobility.

3.5 Summary and conclusions

The presently available methods to simulate spin-label spectra to obtain τ_c values directly provide a sound ranking of the mobility of surface residues.

Fractional solvent accessibility data are well suited to identify residues that are sufficiently exposed for surface labeling. They are less well suited to predict the ranking of mobility, owing to the absence of structural parameters defining the cysteine-spin-label conformations. Here the model of Volkov et al. [6,17] or molecular dynamics approaches [9,13] are more suitable, because they explicitly take the structure of the spin label and its environment into account. The ranking obtained from the Volkov model follows closely the trend in τ_c values, suggesting that this model already reflects the essence of the mobility of the spin labels.

For surface sites, the mobility plot introduced by the Hubbell group [15] does not add much to the τ_c analysis. This derives from the small mobility differences and the errors in the parameters. The mobility plot is better suited to differentiate between spin labels that span the entire range from buried to surface residue and therefore have a larger spread of mobility. The advantage of the plot - to characterize two-component spectra in a single parameter - is partly offset by the small range of those values for sites with close lying mobility.

The disadvantage of τ_c values as a means for mobility ranking is that τ_c and the amount of slow component are interdependent, making the results somewhat dependent on the choices made for the analysis. Also, there is an extensive body of literature using the approach of the Hubbell group to classify spin labels according to their EPR properties. Before a similar collection of τ_c values for different protein types has been established, the Hubbell approach will remain the standard.

Acknowledgments

I would like to acknowledge the following people: dr. Alex Volkov performed the EPR measurements on the mutants T137C, T288C, N200C and N38C and made the calculation for the conformational model. Qamar Bashir prepared the samples. I would like also to thank dr. Marcellus Ubbink for the useful discussions and suggestions.

Reference list

1. Hubbell, W. L.; Altenbach, C. *Current Opinion in Structural Biology* **1994,** *4* (4), 566-573.
2. Hubbell, W. L.; Mchaourab, H. S.; Altenbach, C.; Lietzow, M. A. *Structure* **1996,** *4* (7), 779-783.
3. Hubbell, W. L.; Gross, A.; Langen, R.; Lietzow, M. A. *Current Opinion in Structural Biology* **1998,** *8* (5), 649-656.
4. Finiguerra, M. G.; Blok, H.; Ubbink, M.; Huber, M. *Journal of Magnetic Resonance* **2006,** *180* (2), 197-202.
5. White, G. F.; Ottignon, L.; Georgiou, T.; Kleanthous, C.; Moore, G. R.; Thomson, A. J.; Oganesyan, V. S. *Journal of Magnetic Resonance* **2007,** *185* (2), 191-203.
6. Volkov, A. N.; Worrall, J. A. R.; Holtzmann, E.; Ubbink, M. *Proceedings of the National Academy of Sciences of the United States of America* **2006,** *103* (50), 18945-18950.
7. Isas, J. M.; Langen, R.; Haigler, H. T.; Hubbell, W. L. *Biochemistry* **2002,** *41* (5), 1464-1473.
8. Borbat, P. P.; Mchaourab, H. S.; Freed, J. H. *Journal of the American Chemical Society* **2002,** *124* (19), 5304-5314.
9. Steinhoff, H. J.; Muller, M.; Beier, C.; Pfeiffer, M. *Journal of Molecular Liquids* **2000,** *84* (1), 17-27.
10. Sale, K.; Sar, C.; Sharp, K. A.; Hideg, K.; Fajer, P. G. *Journal of Magnetic Resonance* **2002,** *156* (1), 104-112.
11. Budil, D. E.; Lee, S.; Saxena, S.; Freed, J. H. *Journal of Magnetic Resonance Series A* **1996,** *120* (2), 155-189.
12. Columbus, L.; Kalai, T.; Jeko, J.; Hideg, K.; Hubbell, W. L. *Biochemistry* **2001,** *40* (13), 3828-3846.
13. Steinhoff, H. J.; Hubbell, W. L. *Biophysical Journal* **1996,** *71* (4), 2201-2212.
14. Stoll, S.; Schweiger, A. *Journal of Magnetic Resonance* **2006,** *178* (1), 42-55.
15. Mchaourab, H. S.; Lietzow, M. A.; Hideg, K.; Hubbell, W. L. *Biochemistry* **1996,** *35* (24), 7692-7704.
16. Finiguerra, M. G.; Prudencio, M.; Ubbink, M.; Huber, M. *Magnetic Resonance in Chemistry* **2008,** *46* (12), 1096-1101.

17. Volkov A. Transient Complexes of Haem Proteins. Leiden University, Leiden, Feb 2007.
18. Goodin, D. B.; Davidson, M. G.; Roe, J. A.; Mauk, A. G.; Smith, M. *Biochemistry* **1991,** *30* (20), 4953-4962.
19. Pollock, W. B. R.; Rosell, F. I.; Twitchett, M. B.; Dumont, M. E.; Mauk, A. G. *Biochemistry* **1998,** *37* (17), 6124-6131.
20. Morar, A. S.; Kakouras, D.; Young, G. B.; Boyd, J.; Pielak, G. J. *Journal of Biological Inorganic Chemistry* **1999,** *4* (2), 220-222.
21. Margoliash, E.; Frohwirt, N. *Biochemical Journal* **1959,** *71*, 570-578.
22. Vitello, L. B.; Huang, M.; Erman, J. E. *Biochemistry* **1990,** *29* (18), 4283-4288.
23. Steigmiller, S.; Borsch, M.; Graber, P.; Huber, M. *Biochimica et Biophysica Acta-Bioenergetics* **2005,** *1708* (2), 143-153.
24. Pelletier, H.; Kraut, J. *Science* **1992,** *258* (5089), 1748-1755.
25. Koradi, R.; Billeter, M.; Wuthrich, K. *Journal of Molecular Graphics* **1996,** *14* (1), 51-&.
26. Cavanagh, J.; Fairbrother, W. J.; Palmer III, A. G.; Skelton, N. J. *Protein NMR Spectroscopy: Principles and Practice;* Academic Press: London, 1995.
27. Margittai, M.; Fasshauer, D.; Pabst, S.; Jahn, R.; Langen, R. *Journal of Biological Chemistry* **2001,** *276* (16), 13169-13177.